Theoretical Study of the Proton Transfer of Uracil and (Water)$_n$ (n = 0−4): Water Stabilization and Mutagenicity for Uracil

Xingbang Hu, Haoran Li,* Wanchun Liang, and Shijun Han

Department of Chemistry, Zhejiang University, Hangzhou 310027, PRC

Received: April 28, 2004; In Final Form: June 15, 2004

To investigate the tautomerism of uracil−(water)$_n$ (n = 0−4) that is induced by proton transfer, we describe a study of structural tautomer interconversion and the relative stabilizing influences of water on uracil (U) and its enol form (U*), using density functional theory (DFT) calculations by means of the B3LYP exchange and correlation functions. Thirty-three geometries, including seven significant transition states, were optimized, and their geometrical parameters have been discussed in detail. Water molecules have been gradually placed in different regions in the vicinity of U and U*, and the intermolecular interactions between U, U*, and water molecules have been studied. The relative stabilities of all tautomers were established. The calculated results indicate that there are two absolutely opposite regions in the vicinity of uracil. In one of the regions, water molecules can protect U from tautomerizing to U*, whereas in another region, water molecules can assist the tautomerism from U to U*. The stabilization and mutagenicity effects of increasing the number of water molecules in only one region and in both regions have been systematically studied and discussed.

Introduction

Uracil is a pyrimidine base and a constituent of nucleotides, and as such one member of the base pair AU. It also belongs to a group of the most important pyrimidines that play a fundamental role in the structure and function of enzymes and drugs. Generally, the keto form of uracil exists as the main form in the double helix.[1] The formation of specific AU Watson−Crick hydrogen bonds is responsible for the maintenance of the genetic code. If uracil is replaced by another type of base, it may lead to the introduction of a wrong genetic code. In fact, it has been known for a long time that uracil may also exist in other noncanonical tautomeric forms.[2−4] Some of the tautomeric forms may cause the base mispair, which has been proven to be one of the origins of gene mutation.[2,5,6] Many experiments have been performed to study uracil and its tautomeric forms.[7−13]

Quantum mechanical calculation is an excellent method for producing the precise results of the energetics and geometries of the supermolecules that are formed by a host molecule that is surrounded by explicit water molecules. During the past years, many theoretical studies have been performed to study the interactions of uracil or its tautomeric forms with water. All of the theoretical studies can be classified into two groups. The first group focused primarily on the interaction of uracil and water. Early work performed with correlated calculations by Rybak et al. studied the uracil−water interaction energy at two planar configurations.[14] Smets et al. studied three possible complexes of the uracil with a single water molecule and found that the attachment of the excess electron lowers the relative energy differences among the three complexes.[15] Their further work investigated the ability of the uracil−water complex to form a stable anionic system.[16] Nguyen et al. revealed three favorable sites of a single water molecule in the vicinity of uracil.[17] Ghomi et al. studied the interactions of uracil and two water molecules in order to investigate the effect of the molecular environment on the vibrational dynamics.[18,19] Mourik et al. studied four structures of the uracil−water complex, and two transition-state structures were determined.[20] To obtain more precise results of the energetics and geometries of uracil−(water)$_n$ (n = 1−4) complexes, Mourik et al. developed a more accurate intermolecular potential based on a distributed multipole electrostatic model.[21,22] Dolgounitcheva et al. described the anionic clusters of U and the various numbers of water molecules that are observed in the anion RET experiments[12] and the $(UH_2O)^-$ species that are observed in the anion PES experiments[13] with the electron propagator theory and the many-body perturbation theory.[23] Recently, Gadre et al. studied uracil interacting with water molecules both in square and in cube. They completed a systematic investigation of the clusters that were obtained by the explicit hydration of uracil with electrostatic guidelines as exemplified by the U−$(H_2O)_n$ clusters.[24] Gaigeot et al. studied the geometrical and vibrational properties of uracil−(water)$_n$ (n = 1−7) complexes in an average plane, including uracil.[25,26] Palafox et al. calculated the vibrational frequencies of uracil and the effect of hydration on the uracil.[27] Zhang et al. studied the solvent effects on the internal reorganization energy of the electron transfer of uracil.[28] All of the above work yielded a static picture of the possible and energetically favorable interactions of the uracil−water complexes. A dynamic theoretical analysis of the uracil−water complex at the quantum mechanical level was performed by Gaigeot et al.[29,30] The interaction of uracil and other molecules also received much attention in the past years.[31−35] The second group has primarily studied the relative stability of the tautomeric forms of uracil[36,37] and their interactions with water molecules. There are fewer corresponding theoretical studies of the second group compared to the first group. Kryachko et al. studied twelve tautomeric

* Corresponding author. Fax: +86-571-8795-1895. E-mail: lihr@zju.edu.cn.

10.1021/jp048146y CCC: $27.50
Published on Web 07/29/2004

forms of uracil[4] and their interactions with only one water molecule.[38] The relative order of the stability of the uracil tautomers, in both a monoform and a combination of water molecules, was established.[38]

In summary, all of the above works enhance our perception of the interactions between U/U* and water in the following aspects: different sites of water molecules in the vicinity of U/U*, various numbers of water molecules (from 1 to 7), square and cube models of interactions, and neutral and anion forms of $U-H_2O$. However, the interactions between the U* (the most stable enol form of uracil) and $(H_2O)_n$ ($n = 2-4$) are not reported, and there is a vacancy for the systematical study of the proton-transfer process from $U-(H_2O)_n$ to $U^*-(H_2O)_n$.

It is well-known that nucleic acids are exposed to water solvents in a number of biological structures. Water acts both as a proton acceptor and as a proton donor, and it can affect the structural features that are necessary for the biological functions of nucleic acids. U contains a row of alternating C═O and N−H groups, and U* contains C−O−H, C−O, and C−N groups, which provide a range of possible hydrogen-bonded arrangements for the water molecule. How does water affect the relative stability of U and U*? What role does water play in the tautomerism process from U to U*? The present work will address these questions and focus on the following aspects: (i) give precise results of the energetics and geometries of $U^*-(H_2O)_n$ ($n = 2-4$); (ii) investigate the proton-transfer processes from $U-(H_2O)_n$ to $U^*-(H_2O)_n$ ($n = 1-4$), and determine some of the transition states in these courses; and (iii) find the differences when water molecules are located in different regions in the vicinity of U and U*.

Computational Methods

Gaigeot et al. had shown in detail that DFT and MP2 levels of theory gave similar results for the geometrical and vibrational features of the nucleic acid base in which they were interested.[11,39] Therefore, we optimized the structures of uracil−(water)$_n$ and tautomer−(water)$_n$ ($n = 1-4$) complexes at the B3LYP/6-31+G* level of theory. Energy, frequency calculation, and zero-point energy (ZPE) corrections have been performed at the same level of theory.

The computed stationary points have been characterized as minima or transition states by diagonalizing the Hessian matrix and analyzing the vibrational normal modes. In this way, the stationary points can be classified as minima if no imaginary frequencies are shown or as transition states if only one imaginary frequency is obtained.[40,41] The particular nature of the transition states has been determined by analyzing the motion described by the eigenvector associated with the imaginary frequency.

The effect of the basis set superposition error (BSSE) has been analyzed by means of the counterpoise correction method.[42] The energy of binding uracil to water molecules has been determined by[25,43]

$$\Delta E_{BE}^{MW} = E_{M-n(W)} - E_M - \sum E_{n(bW)}$$

Here, W and bW denote free water and the best cluster containing n water molecules, respectively. A negative value of ΔE_{BE}^{MW} indicates that the molecule can interact favorably with the corresponding most stable $(H_2O)_n$ cluster.[43]

All calculations have been performed with the Gaussian 98 suite of programs.[44]

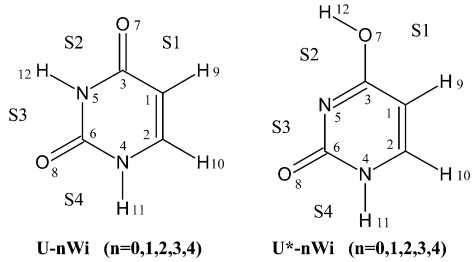

Figure 1. Preferential sites of water molecules in the vicinity of uracil and its tautomer U*. S1, S2, S3, and S4 represent the favorable regions for water molecules.

Results and Discussion

Although uracil has many tautomeric forms, among normal nucleobases, U* (Figure 1) is the most stable form.[4,38] Hence, we give more attention to the interactions of $U^*-(H_2O)_n$ ($n = 1-4$) and mainly focus on the proton-transfer process from $U-(H_2O)_n$ to $U^*-(H_2O)_n$ ($n = 1-4$). In the present work, in the vicinity of uracil, four favorable regions, S1, S2, S3, and S4, for water molecules (Figure 1) are taken into consideration. It is worth noticing that if water acts both as a proton acceptor and as a proton donor, the relevant structure is energetically favored over the alternative double-donor or double-acceptor hydrogen bonding.[38,45] Therefore, we consider water as an H-bond acceptor or donor via the interactions occurring through its oxygen or hydrogen atoms, respectively.

1. The Tautomerization Process from Isolated Uracil to Its Tautomer U*. The optimized geometrical parameters of these compounds are listed in Table 1. Our results agree well with not only the recent geometrical optimizations of uracil at the MP2/6-311G*[20] and CP-MD simulations[29] but also those obtained by X-ray[46] and electron diffraction.[47] The optimized geometrical parameters of U* show good agreement with recent B3LYP/6-31G** calculations.[4] The relative free-energy change of base tautomerism from the keto form to the enol form is listed in the first line of Table 2. The result shows clearly that the keto form is more stable than the enol form, which is in agreement with Orozco's theoretical study.[36]

The proton transfer proceeds from isolated U to U* via a transition state of Uts (Figure 4). This transition state possesses an imaginary frequency (1918i cm^{-1}) assigned to the single-proton transfer of H12. The greatest changes of geometrical parameters in the tautomerism processes are those relating to the O7−C3−N5 bonds. The C3−O7 bond lengths of U, Uts, and U* are 1.223, 1.284, and 1.345 Å, respectively. It is worth noticing that to reach Uts, the C1−C3−O7 angle becomes flexural from 126.08 to 131.83° and then is reduced from 131.83 to 116.40°. Such a process makes the proton transfer difficult, which has been proven by the high barrier of 178.68 kJ/mol.

2. The Tautomerism Process from $U-(H_2O)_n$ to $U^*-(H_2O)_n$ ($n = 1-4$). In fact, many structural features that are necessary for the biological functions of nucleic acids depend on their interactions with surrounding water. For this reason, we also adopted an energy change for investigating the role of water in the tautomerism process. The energetic perspective has been successfully used for studying the spontaneous DNA mutation that is induced by proton transfer.[36,48,49]

In the vicinity of the U and U*, four different regions for water molecules (S1, S2, S3, and S4 in Figure 1) were taken into consideration. The free-energy changes of the tautomerism processes are listed in Table 2. It can be concluded that even though the interaction with water is considered, it does not

TABLE 1: Geometrical Parameters of U, Uts, and U*

	U					Uts	U*
	this work	MP2/6-311G*[a]	CP-MD[b]	exp[c]	exp[d]	this work	this work
bond							
C1═C2	1.352	1.353	1.354	1.340	1.343	1.367	1.363
C1−C3	1.459	1.460	1.460	1.430	1.462	1.425	1.430
C1−H9	1.082	1.082	1.085	0.970	1.072	1.081	1.082
C2−N4	1.377	1.375	1.382	1.359	1.399	1.362	1.358
C2−H10	1.085	1.085	1.088	0.957	1.072	1.086	1.085
C3−N5	1.412	1.408	1.428	1.371	1.399	1.353	1.308
C3═O7	1.223	1.218	1.233	1.245	1.212	1.284	1.345
N4−C6	1.394	1.390	1.406	1.371	1.399	1.428	1.424
N4−H11	1.012	1.008	1.020	0.836	1.002	1.013	1.013
N5−C6	1.385	1.385	1.393	1.377	1.399	1.371	1.380
C6═O8	1.220	1.214	1.229	1.215	1.212	1.217	1.221
N5−H12	1.015	1.012	1.024	0.877	1.002	1.338	2.253
O7−H12						1.341	0.977
angle							
N5−C3−C1	113.68	113.15	113.4	115.5	115.5	122.29	125.58
N5−C3═O7	120.23	120.70	119.9	119.2	120.2	105.87	118.01
C3−O7−H12	56.38					76.35	106.82
C3−N5−H12	116.37	115.91	116.1	115.5	116.1	74.18	56.38
C1−C3═O7	126.08	126.15	126.6	125.3	124.3	131.83	116.41
C3−C1−H9	118.17	118.46	118.1	118.1	118.9	122.53	121.83

[a] Calculated at MP2/6-311G* (ref 20). [b] Car−Parrinello MD simulation results (ref 29). [c] Experimental values from X-ray (ref 46). [d] Experimental values from electron diffraction (ref 47).

TABLE 2: Free-Energy Changes (kJ/mol) and Equilibrium Constants of Uracil−Water Tautomerism[a]

tautomerism	ΔG	$\Delta(\Delta G)$[b]	K_{eq}[c]
U → U*	55.09	0.00	2.23×10^{-10}
U−W1 → U*−W1	63.77 (63.88)	8.68 (8.79)	6.43×10^{-12}
U−W2 → U*−W2	42.90 (41.66)	−12.19 (−13.43)	5.02×10^{-8}
U−W3 → U*−W3	53.75 (54.26)	−1.34 (−0.83)	3.12×10^{-10}
U−W4 → U*−W4	51.94 (51.62)	−3.15 (−3.47)	9.04×10^{-10}
U−2W1 → U*−2W1	69.47 (69.68)	14.38 (14.59)	6.19×10^{-13}
U−W1−W2 → U*−W1−W2	49.71 (50.22)	−5.38 (−4.87)	1.59×10^{-9}
U−2W2 → U*−2W2	39.28 (34.21)	−15.81 (−20.88)	1.01×10^{-6}
U−3W1 → U*−3W1	73.65 (74.09)	18.56 (19.00)	1.05×10^{-13}
U−2W1−W2 → U*−2W1−W2	53.10 (54.38)	−1.99 (−0.71)	2.97×10^{-10}
U−W1−2W2 → U*−W1−2W2	43.30 (41.58)	−11.79 (−13.51)	5.19×10^{-8}
U−3W2 → U*−3W2	37.72 (31.91)	−17.37 (−23.18)	2.57×10^{-6}
U−3W1−W2 → U*−3W1−W2	54.15 (55.92)	−0.94 (0.83)	1.59×10^{-10}
U−2W1−2W2 → U*−2W1−2W2	43.19 (42.41)	−11.90 (−12.68)	3.71×10^{-8}
U−W1−3W2 → U*−W1−3W2	41.88 (37.77)	−13.21 (−17.32)	2.41×10^{-7}

[a] The values in parentheses indicate the free-energy changes with BSSE correction. [b] $\Delta(\Delta G) = \Delta G_{(U-nW1-mW2 \rightarrow U^*-nW1-mW2)} - \Delta G_{(U \rightarrow U^*)}$, ($n = 0-3$, $m = 0-3$). [c] Equilibrium constants were calculated (ref 55) using free-energy changes with BSSE correction at 298.15 K.

change the main form of uracil. Our results qualitatively agree well with the experimental evidence, which shows that the enol forms of uracil derivatives are present in a minority population in water.[50,51] However, it is worth noticing that water does affect the tautomerization process from U−$(H_2O)_n$ to U*−$(H_2O)_n$. How the water on different sites affected the tautomerism process was studied in detail.

As the results show in Table 3, though there are considerable differences in the binding energy of U/U* and water molecules, the negative values of ΔE_{BE}^{MW} indicate that water can interact favorably with U or U* in all of our selected regions (S1, S2, S3, and S4). The relative order of stability of U + $1H_2O$ is U−W4 > U−W2 > U−W3 > U−W1 (W1, W2, W3, and W4 represents a single water molecule in S1, S2, S3, and S4, respectively), which is in agreement with that obtained at the MP2/6-311++G**[23] and B3LYP/6-31++G* levels.[25] The relative order of stability of U* + $1H_2O$ is U*−W2 > U*−W4 > U*−W3 > U*−W1. Although water molecules in S3 and S4 attain considerable binding energy when they interact with U or U*, they change the free energy of the tautomerization only slightly compared to the isolated tautomerization of U → U* (Table 2). Hence, when we studied the influences that were induced by more than one water molecule, S3 and S4 were not discussed in detail. On the other hand, water molecules in S1 and S2 change the free energy significantly, and the effects that were induced by the explicit water molecules in S1 and S2 should not be neglected.

*2.1. Water Molecules Located in Region S1 Can Protect U from Tautomerizing to U**. In this part, water molecules have been gradually placed in S1 and six different configurations with water molecules in this region were optimized (Figure 2).

When a single water molecule (W1) is located in S1, water acts as an H-bond donor. Some pioneering papers indicated that water in S1 could also act as a weak H-bond acceptor.[16,20−26,28,38] However, recent CP-MD results contributed by Gaigeot et al. argued against the existence of the C1−H9···O(W1) weak hydrogen bond in region S1.[29,30] Because the CP-MD results describe a more realistic model system, we do not take the C1−H9···O(W1) hydrogen bond into consideration in this work; we only consider the W1 hydrogen bonds to C3−O7. To show the position change of water in S1 during the tautomerism process from U to U* conveniently, we draw a dashed line that connects

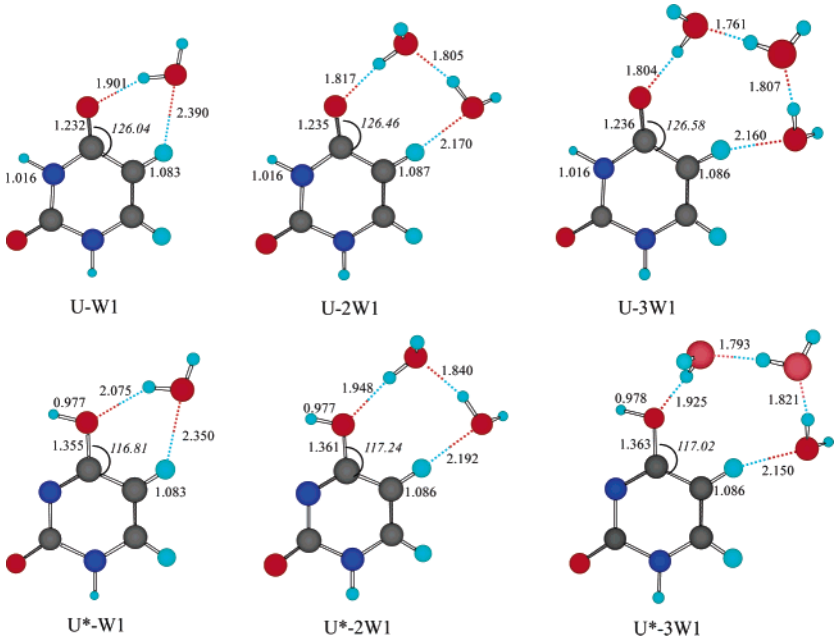

Figure 2. Optimized structures with water molecules in S1, calculated at the B3LYP/6-31+G(d) level. The number values shown refer to computed bond distances and intramolecular angles.

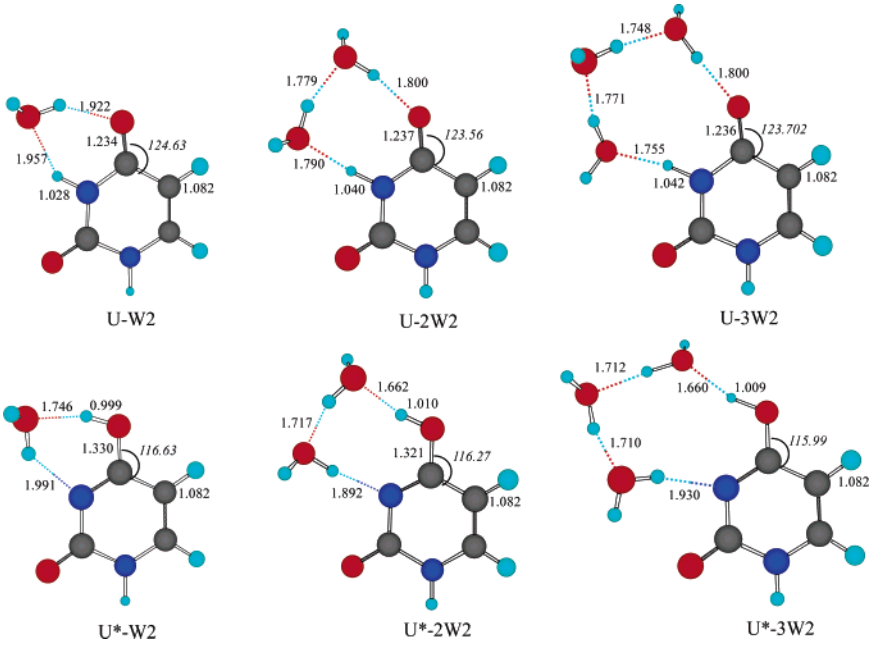

Figure 3. Optimized structures with water molecules in S2, calculated at the B3LYP/6-31+G(d) level. The number values shown refer to computed bond distances and intramolecular angles.

C1−H9 with O(W1). When we compare the isolated U and U*, the C3−O7 bonds in both U−W1 and U*−W1 are lengthened. However, water in S1 does not change the effect of O7−H12 in U* at all. Since the formation of the hydrogen bond O7···H−O(W1) changes the electron density around O7, the tautomerization process of U−W1 → U*−W1 becomes more difficult than that of U → U*. This has been proven by the increment in the free-energy change of 8.79 kJ/mol. The equilibrium constant for the tautomerism of U−W1 → U*−W1 is 35 times less than that of U → U* (Table 2). Videlicet, the water located in the region of S1 can protect U from tautomerizing to U*.

When a water monomer is replaced by a water dimer in S1, considerable shortening of the C3═O7···H(W1) bonds and reasonable lengthening of the C3−O7 bond are observed. A water dimer located in S1 reinforces the protection effect of the tautomerism from U to U*, which has been proven by the increment in the free-energy change of 14.59 kJ/mol. The equilibrium constant for the tautomerism of U−2W1 → U*−2W1 is 360 times less than that of U → U* (Table 2).

It is not surprising that when a water trimer is located in the S1 region, the protection effect that is induced by the water trimer is greater than that of both the water monomer and the water dimer in S1. The equilibrium constant for the tautomerism of U−3W1 → U*−3W1 is 2.13×10^3 times less than that of U → U* (Table 2). There is also a corresponding shortening of the C3═O7···H(W1) hydrogen bond compared with the bond lengths of U−2W1 and U*−2W1.

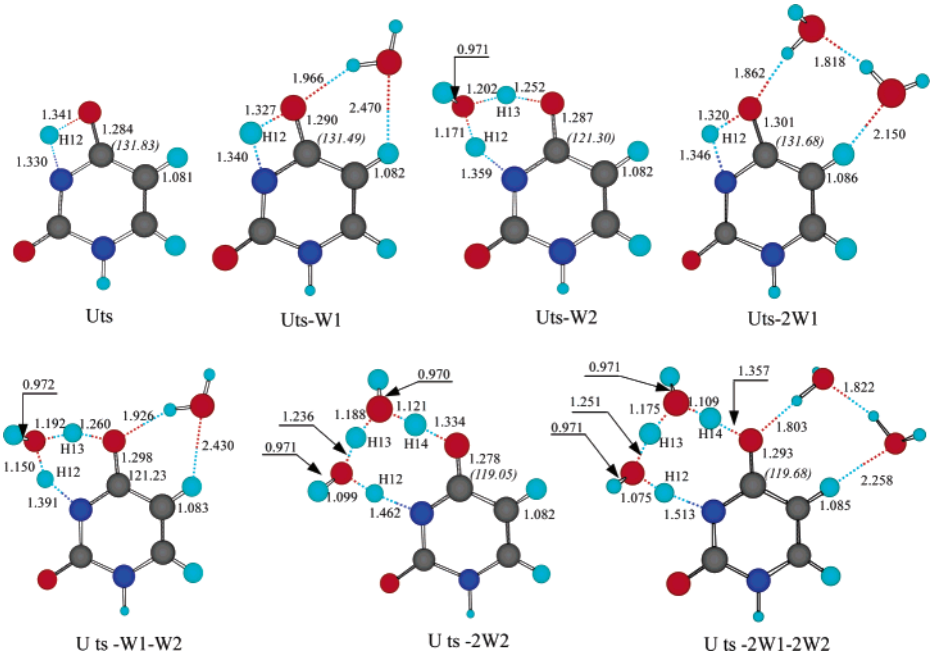

Figure 4. Related transition states with single, double, and tripartite proton transfer of the tautomerization process $U-(H_2O)_n \rightarrow U^*-(H_2O)_n$, calculated at the B3LYP/6-31+G(d) level. The number values shown refer to computed bond distances and intramolecular angles.

TABLE 3: Binding Energies (kJ/mol) of U/U* to Water Molecules[a]

compd	ΔE_{BE}^{MW}	compd	ΔE_{BE}^{MW}
U−W1	−24.86 (−25.06) −25.33[b]	U*−W4	−43.67 (−44.90)
U−W2	−33.11 (−33.89) −33.46[c]	U−2W1	−42.38 (−42.63)
U−W3	−30.30 (−31.05) −31.83[c]	U−W1−W2	−56.79 (−58.60)
U−W4	−39.68 (−40.54) −40.03[c]	U−2W2	−57.62 (−59.84)
U*−W1	−12.83 (−12.98)	U*−2W1	−24.75 (−24.77)
U*−W2	−47.09 (−49.07)	U*−W1−W2	−62.70 (−63.93)
U*−W3	−22.35 (−22.77)	U*−2W2	−77.22 (−82.91)

[a] The values outside of the parentheses indicate the binding energies with BSSE correction. [b] Calculated at MP2/DZPi (ref 20). [c] Calculated at MP2/ESPB (ref 20).

It should be noticed that the energy changes in the tautomerism of U−3W1 → U*−3W1 cannot be considered as a simple superposition of those in U−W1 and U−2W1. We could see that the order of the decrease of the free-energy change is

$$\text{U}-3\text{W1} \rightarrow \text{U}^*-3\text{W1} \quad \underset{(4.41\ \text{kJ/mol})}{\overset{4.18\ \text{kJ/mol}}{>}}$$

$$\text{U}-2\text{W1} \rightarrow \text{U}^*-2\text{W1} \quad \underset{(5.80\ \text{kJ/mol})}{\overset{5.70\ \text{kJ/mol}}{>}}$$

$$\text{U}-\text{W1} \rightarrow \text{U}^*-\text{W1} \quad \underset{(8.79\ \text{kJ/mol})}{\overset{8.68\ \text{kJ/mol}}{>}} \quad \text{U} \rightarrow \text{U}^*$$

The values above the sign of inequality equal the quantity of the left side of the sign minus that of the right side. The values in the parentheses are the corresponding values with BSSE corrections. This indicates that the water molecules that are located in S1 can protect U from tautomerizing to U*. As the number of water molecules in S1 increases from 1 to 3, the protection ability is reinforced, but the extent of the increment of the free-energy change is reduced.

The proton-transfer processes of U−W1 → U*−W1 via a transition state Uts−W1 (Figure 4) possesses an imaginary frequency of 1911i cm^{-1}, and the process of U−2W1 → U*−2W1 via a transition state Uts−2W1 (Figure 4) possesses an imaginary frequency of 1900i cm^{-1}. The imaginary frequency is assigned to the single proton transfer of H12. As in the proton-transfer process of U → U*, the geometrical configuration around O7−C3−N5 changes significantly in the tautomerizing process with water molecules in S1. The value of the C1−C3−O7 angle is increased at first and then decreased in the tautomerizing process. The C3−O7 bond is lengthened in the whole tautomerizing process. The values of the C3−O7 bond lengths are 1.232, 1.290, and 1.355 Å in U−W1 → Uts−W1 → U*−W1 and 1.235, 1.301, and 1.361 Å in U−2W1 → Uts−2W1 → U*−2W1, respectively. As the number of water molecules in S1 increases from 0 to 2, the C3−O7 bond correspondingly lengthens. It is worth noticing that during the same course, the N5···H12 bond angle in the transition state increases dramatically. It may lead to an augmentation of the activation energy. The order of the decrease in the activation energy is

$$\text{Uts}-2\text{W1} \quad \underset{>}{\overset{0.11\ \text{kJ/mol}}{}} \quad \text{Uts}-\text{W1} \quad \underset{>}{\overset{2.76\ \text{kJ/mol}}{}} \quad \text{Uts}$$

It reveals that water molecules located in S1 can increase the activation energy of the U → U* process. As the number of water molecules in S1 increases from 0 to 2, the barrier is heightened, but the extent of the increment of the activation energy is reduced.

As discussed above, the following can be safely stated: water molecules in S1 can protect U from tautomerizing to U* in both thermodynamics and dynamics.

*2.2. Water Molecules Located in Region S2 Can Assist the Tautomerizing Process from U to U**. As they were in section 2.1, water molecules have been gradually placed in S2. In total, six different configurations with water molecules in S2 were optimized (Figure 3).

Water molecules in S2 play a completely opposite role than those in S1.When a single water molecule (W2) is located in S2, water acts as an H-bond acceptor and donor, simultaneously. In the tautomerism of U−W2 → U*−W2, water accepts the

hydrogen atom from the N5−H12 bond of U; at the same time, it donates its hydrogen atom to U, which is accepted by O7. Unlike U−W1 and U*−W1, the C3−O7 bonds in U−W2 are lengthened compared with those of U, while the C3−O7 bonds in U*−W2 are shortened compared with those of U*. Furthermore, the O7−H12 bond in U*−W2 is longer than that of U*. Moreover, the water located in S2 increases the partial electron density surrounding O7 in U and U* significantly, which makes the O7 of U susceptible to attack by the proton. Hence, it is not surprising that W2 can decrease the free-energy change of tautomerization by 13.43 kJ/mol compared with the U → U* transfer (Table 2). When we compared the free-energy change with U−W1 → U*−W1, the decreased value was 22.22 kJ/mol. The equilibrium constant for the tautomerism of U−W2 → U*−W2 is 225 times larger than that of U → U* and 7.81 × 10^3 times larger than that of U−W1 → U*−W1 (Table 2). That is to say, W2 makes U* more stable than isolated U* and assists in the tautomerization of U → U*.

When a water monomer is replaced by a water dimer in S2, considerably shortened bond lengths of C3═O7···H(W) and N5−H12···O(W) in U−2W2 and N5···H−O(W) in U*−2W2 hydrogen bonds are observed. The C3−O7 bond in U−W2 is relengthened, and the C3−O7 bond in U*−W2 is reshortened. Accordingly, a water dimer in S2 reinforces the assisting effect on the tautomerism from U to U*, which has been proven by the decrease of the free-energy change by 20.88 kJ/mol. The equilibrium constant for the tautomerism of U−2W2 → U*−2W2 is 4.53 × 10^3 times larger than that of U → U* and 1.63 × 10^6 times larger than that of U−2W1 → U*−2W1 (Table 2).

When a water dimer is replaced by a water trimer in the S2 region, only a small shortening of the O7−H12···O(W) and N5−H12···O(W) hydrogen bonds in U−3W2 is observed. C3−O7 bonds and C3═O7···H(W) hydrogen bonds compared with those in U−2W2 and U*−2W2 almost do not change. Accordingly, the assisting effect on the tautomerism induced by a water trimer in S2 is similar to that in the water dimer in S2.

The order of the increase of the free-energy change is

$$\text{U}-3\text{W2} \rightarrow \text{U}^*-3\text{W2} \overset{1.56\ \text{kJ/mol}}{<} (2.3\ \text{kJ/mol})$$

$$\text{U}-2\text{W2} \rightarrow \text{U}^*-2\text{W2} \overset{3.62\ \text{kJ/mol}}{<} (7.45\ \text{kJ/mol})$$

$$\text{U}-\text{W2} \rightarrow \text{U}^*-\text{W2} \overset{12.19\ \text{kJ/mol}}{<} (13.43\ \text{kJ/mol}) \quad \text{U} \rightarrow \text{U}^*$$

It indicates that water molecules located in S2 can assist in the tautomerizing of U → U*. With the increase in the number of water molecules in S2 from 1 to 3, the assisting ability is reinforced, whereas the extent of the decrease in the free-energy change is lessened.

In the proton-transfer process of U−W2 → U*−W2, H12 is delocalized from U and H13 is delocalized from W2. The process via a transition state of Uts−W2 (Figure 4) possesses an imaginary frequency of 1552i cm^{-1} assigned to the simultaneous double-proton transfer of H12 and H13. It can be seen that there is a hexahydric ring in the Uts−W2 state, in which water acts as a bridge. The bond lengths vary from 1.17 to 1.35 Å in the ring. Obviously, this ring makes the tautomerization from U−W2 to U*−W2 possible with just a small change in the C1−C3−O7 angle. It is worth noticing that the value of the C1−C3−O7 angle decreases in the whole tautomerizing process, while in the tautomerism of U → U*, this value increases at first and then decreases. The formation of the hexahydric ring lowers the activation energy considerably, which makes the rate constant of U−W2 → U*−W2 4.55 × 10^{17} times faster than that of U → U*.

TABLE 4: Activation Energy (kJ/mol) and Rate Constant (s^{-1}) of Uracil−Water Tautomerism

tautomerism	$\Delta G^{\ddagger}$	k^a
U → U*	178.68	3.08 × 10^{-19}
U−W1 → U*−W1	181.44	1.01 × 10^{-19}
U−W2 → U*−W2	77.94	0.14
U−2W1 → U*−2W1	181.55	9.67 × 10^{-20}
U−W1−W2 → U*−W1−W2	80.86	0.04
U−2W2 → U*−2W2	71.32	1.99
U−2W1−2W2 → U*−2W1−2W2	73.60	0.79

[a] Values were estimated at 298.15 K by using the transition-state theory (refs 56 and 57).

TABLE 5: Some Significant Donor−Acceptor Natural Bond Orbital Interactions of U/U* and W1/W2 and Their Second-Order Perturbation Stabilization Energies (kJ/mol)[a]

donor	acceptor	inter-actions	ΔE_2
U−W1: from U to W1			
LP(1) O7	BD*(1) O(W1)−H(W1)	n → σ^*	14.63
LP(2) O7	BD*(1) O(W1)−H(W1)	n → σ^*	36.62
U*−W1: from U* to W1			
LP(1) O7	BD*(1) O(W1)−H(W1)	n → σ^*	19.52
U−W2: from U to W2			
LP(1) O7	BD*(1) O(W2)−H(W2)	n → σ^*	14.34
LP(2) O7	BD*(1) O(W2)−H(W2)	n → σ^*	33.48
U−W2: from W2 to U			
BD(1) O(W2)−H(W2)	BD*(1) N5−H12	σ → σ^*	4.31
LP (2) O(W2)	BD*(1) N5−H12	n → σ^*	50.12
U*−W2: from U* to W2			
LP(1) N5	BD*(1) O(W2)−H(W2)	n → σ^*	49.24
U*−W2: from W2 to U*			
BD(1) O(W2)−H(W2)	BD*(1) O7−H12	σ → σ^*	8.36
LP(2) O(W2)	BD*(1) O7−H12	n → σ^*	102.66

[a] NBO analyses were performed at B3LYP/6-31+G* levels of theory. BD denotes the occupied bond orbital, and BD* denotes the formally empty antibonding orbital. LP denotes the occupied lone pair. ΔE_2 is calculated as the same formula given in ref 58.

The proton-transfer process of U−2W2 → U*−2W2 via a transition state of Uts−W2 (Figure 4) possesses an imaginary frequency of 1116i cm^{-1} assigned to the simultaneous tripartite proton transfer of H12, H13, and H14. Water molecules in S2 can decrease the activation energy of U → U* with the relative order

$$\text{Uts}-2\text{W2} \overset{6.62\ \text{kJ/mol}}{<} \text{Uts}-\text{W2} \overset{100.74\ \text{kJ/mol}}{\ll} \text{Uts}$$

Consequently, from both thermodynamic and dynamic points of view, we can draw a conclusion that water molecules in S2 can assist in the tautomerizing of U → U*.

Why can water in different regions affect the tautomerizing of U → U* contrarily? Some molecular explanations from natural bond orbital (NBO) analyses and molecular orbitals analyses are given.

The NBO analysis can give some insights into the stabilization that is induced by the donor−acceptor natural bond orbital interactions. As shown in Table 5, the tautomerism process from U to U* weakens the interactions of n → σ^* between U/U*

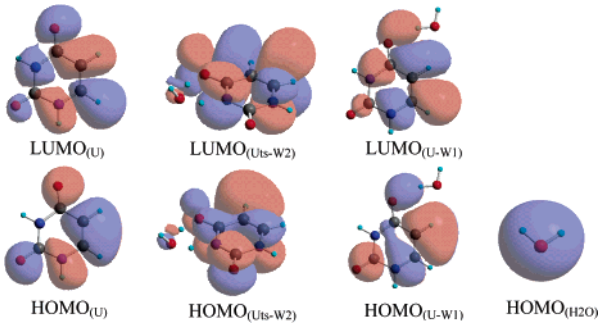

Figure 5. Some important LUMO and HOMO, calculated at the B3LYP/6-31+G* levels.

and W1, whereas it enhances the interactions of n → σ^* and $\sigma \rightarrow \sigma^*$ between U/U* and W2. Hence, it is reasonable that the equilibrium is more favorable to U in the U−W1 → U*−W1 process and contrarily more favorable to U* in the U−W2 → U*−W2 process.

Some important lowest-unoccupied molecular orbitals (LUMO) and highest-occupied molecular orbitals (HOMO) are presented in Figure 5. For the $U_{isolated} \rightarrow U^*_{isolated}$ or U−W1 → U*−W1 process, N5−H12 is the electron acceptor and C3═O7 is the electron donor. As we can see, the LUMO of the electron acceptor does not have the same symmetry as the HOMO of the electron donor, and the energy gap between the LUMO and HOMO is large (0.206 Hartree for U). Hence, it is difficult for isolated U to tautomerize to U*. Furthermore, compared to the HOMO of U, the p orbital of O7 of the U−W1 deviates slightly from the center and moves toward W1, which will lengthen the protron-transfer distance. It leads to a moderate increment of the active energy of the U−W1 → U*−W1 transfer compared to that of U → U*.

However, when a water molecule appears in the S2 region, the water acts as a bridge that can assist the tautomerism process. At first, N5−H12 is the electron acceptor and O(W2) is the electron donor. As we can see, the LUMO of the electron acceptor has the same symmetry as the HOMO of the electron donor. Furthermore, for the transition state (Uts−W2) of the tautomerism process, H12 and H(W2) are electron acceptors and O(W2) and O(7) are electron donors. It is clear that the LUMO of the electron acceptor H12 has the same symmetry as the HOMO of the electron donor O(W2). It is also symmetrically allowable for H(W2) and O(7). Hence, W2 can assist the tautomerism process.

2.3. Tautomerism with Water Molecules in both S1 and S2. In this part, we place water molecules in both S1 and S2, one by one. Twelve different configurations with water molecules in both S1 and S2 are optimized (Figure 6).

It should be noticed that the energy change in the tautomerism with water in both S1 and S2 cannot be considered as a simple superposition of that in S1 and S2. It can be seen that water molecules in S2 have a stronger effect than those in S1. At the same time, the protection effect induced by the water molecules in S1 could not be ignored. When a single water molecule is located in S2, a water monomer in S1 increases the free-energy change by 8.56 kJ/mol and a water dimer in S1 increases the free-energy change by 12.72 kJ/mol. When a water dimer is located in S2, a water monomer in S1 only increases the free-energy change by 7.37 kJ/mol and a water dimer in S1 increases the free-energy change by 8.20 kJ/mol.

Without BSSE correction, a single water molecule in S2 always makes the free-energy change lower than that of the U → U* process, though the number of water molecules in S1 increases from 1 to 3:

$$\mathrm{U} \rightarrow \mathrm{U}^* \overset{0.94\ \mathrm{kJ/mol}}{>} \mathrm{U{-}3W1{-}W2} \rightarrow$$

$$\mathrm{U^*{-}3W1{-}W2} \overset{1.05\ \mathrm{kJ/mol}}{>} \underset{(1.54\ \mathrm{kJ/mol})}{\mathrm{U{-}2W1{-}W2} \rightarrow}$$

$$\mathrm{U^*{-}2W1{-}W2} \overset{3.39\ \mathrm{kJ/mol}}{>} \underset{(4.16\ \mathrm{kJ/mol})}{\mathrm{U{-}W1{-}W2} \rightarrow}$$

$$\mathrm{U^*{-}W1{-}W2}$$

However, when BSSE correction is taken into account, the corresponding order should be changed as follows:

$$\mathrm{U{-}3W1{-}W2} \rightarrow \mathrm{U^*{-}3W1{-}W2} \underset{(0.83\ \mathrm{kJ/mol})}{>} \mathrm{U} \rightarrow$$

$$\mathrm{U^*} \overset{1.05\ \mathrm{kJ/mol}}{>} \underset{(1.54\ \mathrm{kJ/mol})}{\mathrm{U{-}2W1{-}W2} \rightarrow}$$

$$\mathrm{U^*{-}2W1{-}W2} \overset{3.39\ \mathrm{kJ/mol}}{>} \underset{(4.16\ \mathrm{kJ/mol})}{\mathrm{U{-}W1{-}W2} \rightarrow}$$

$$\mathrm{U^*{-}W1{-}W2}$$

In the proton-transfer process of U−W1−W2 → U*−W1−W2, H12 is delocalized from U and H13 is delocalized from W2. This transfer proceeds via a transition state of Uts−W1−W2 with an imaginary frequency of 1460i cm^{-1} that is assigned to the simultaneous double-proton transfer. The tautomerism of U−2W1−2W2 → U*−2W1−2W2 via a transition state of Uts−2W1−2W2 possesses an imaginary frequency of 926i cm^{-1} that is assigned to the tripartite-proton transfer of H12, H13, and H14 (Figure 4). The hydrogen bonds of N5−H12···O(W2) and O7···H−O(W2), which are weak in the minimum energy form of U−W1−W2, become much stronger in the related transition state, whereas the hydrogen bond of O7···H−O(W1), which is rather weak in U−W1−W2, becomes even weaker in the transition state. According to our calculated results, the activation energy of U−*n*W1−*n*W2 → U*−*n*W1−*n*W2 can be regarded simply as a superposition of that of U−*n*W1 → U*−*n*W1 and U−*n*W2 → U*−*n*W2 ($n = 1$ or 2). A single water molecule located in S1 increases the activation energy by 2.76 kJ/mol, and a single water molecule in S2 lowers the activation energy by 100.74 kJ/mol. Hence, we can derive the result that a single water molecule in S1 and another one in S2 should decrease the activation energy by 97.98 kJ/mol (the corresponding DFT calculation result is 97.82 kJ/mol). Similarly, we can see that a water dimer in S1, together with a water dimer in S2, should decrease the activation energy by 104.48 kJ/mol (the corresponding DFT calculation result is 105.08 kJ/mol).

Conclusions

To investigate the structural tautomer interconversion of uracil that is induced by proton transfer, we have studied the interaction of U/U* with $(water)_n$ ($n = 0-4$). Twenty-four complexes of uracil tautomers with water molecules have been chosen for this purpose. Seven significant transition states in the related proton-transfer processes have also been studied. On the basis of the results that were obtained from our calculations, the following can be stated:

(1) There are two absolutely opposite regions in the vicinity of uracil. In the S1 region, water molecules can protect U from

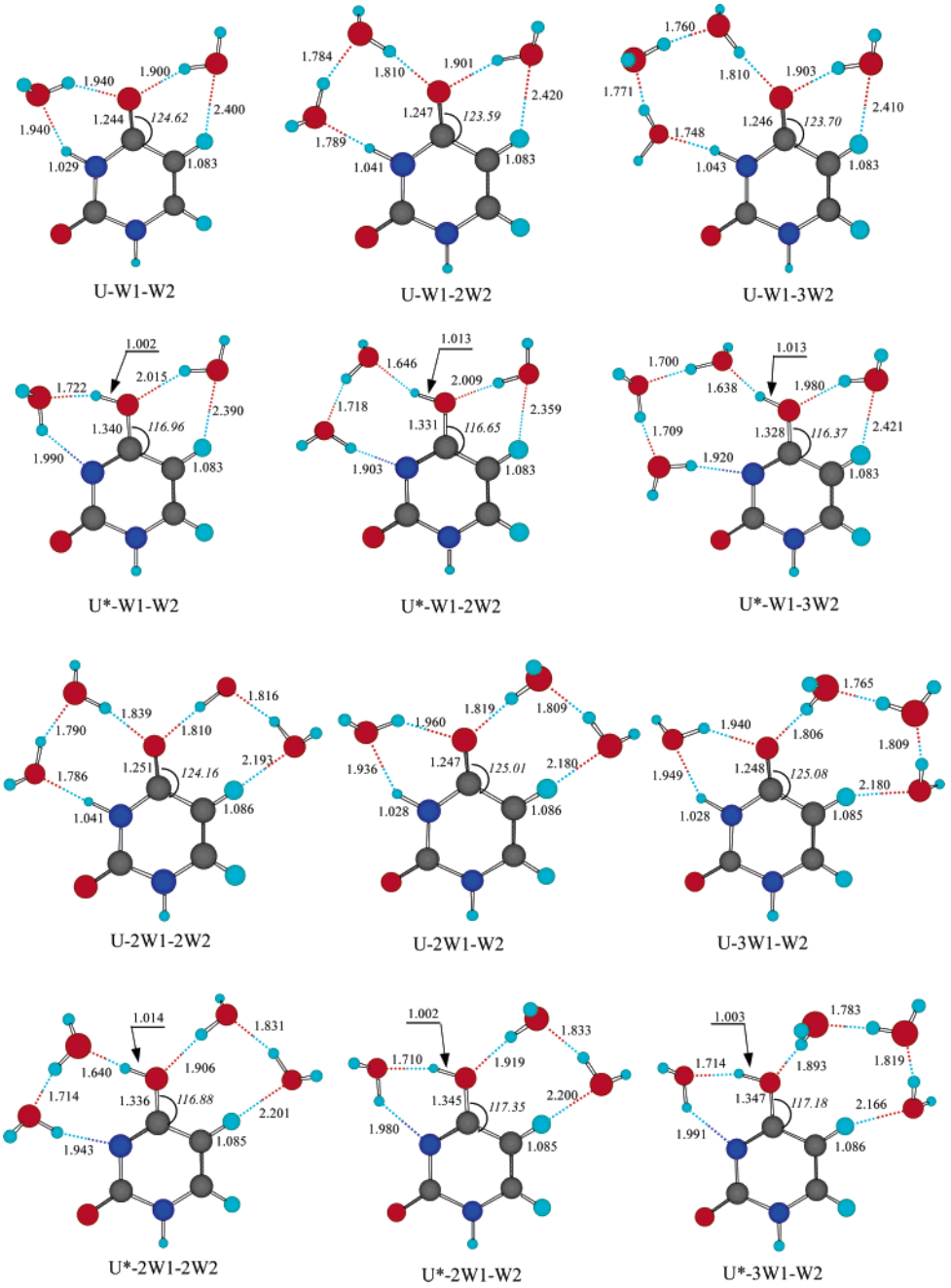

Figure 6. Optimized structures with water molecules in both S1 and S2, calculated at the B3LYP/6-31+G(d) level. The number values shown refer to computed bond distances and intramolecular angles.

tautomerizing to U*. However, in the S2 region, water molecules can assist the tautomerism from U to U*. These results are credible from both thermodynamics and dynamics points of view. A water trimer in S1 can decrease the equilibrium constant of U → U* by 2.13×10^3 times. A water trimer in S2 can increase the equilibrium constant of U → U* by 1.15×10^4 times.

(2) As the number of water molecules located in the S1 region increases from 0 to 3, the protection ability that hinders the tautomerism is reinforced. Similarly, as the number of water molecules located in the S2 region increases from 0 to 3, the assisting tautomerism ability becomes stronger.

(3) When water molecules are located in both S1 and S2, the water molecules in the S2 region play a dominating role in the tautomerism process and water molecules in the S1 region play a subordinate role, but the opposite role induced by the water molecules in S1 can never be ignored.

Furthermore, our water stabilization and mutagenicity concept may indicate a new mechanism of the origin of the mutagenicity of 5-bromouracil (BrU). It is widely accepted that the mutagenic action of BrU is based on enolization and ionization. A conventional viewpoint of enolization is that the presence of the bromine at position 5 significantly alters the distribution of electrons in the base so that BrU can spend part of its existence in the rare enol form.[52] However, this concept encountered challenges from Orozco and co-workers.[36] On the basis of the calculated results which show that BrU has similar stability with U, Orozco et al. suggested that the mutagenic effect of BrU was due to its ability to lose a proton at N5 rather than its tendency to form enol tautomers. According to our water stabilization and mutagenicity concept, we can put forward another mechanism on the enolization of BrU and the following can be predicted; because of the volume and the electron effect of bromine, it becomes difficult for water molecules to enter

the S1 region of BrU. That is to say, the bromine substitution at position 5 of U will lead to the loss of protection induced by water molecules in the S1 region. Accordingly, the likelihood of tautomerism from BrU to BrU* will be much higher than that of U to U*. It has been widely accepted that the existence of the enol tautomer of 5-bromouracil is the origin of its mutagenic property.[2,53,54] Our present work will give a base for the further work on the mechanism of the enolization of BrU.

Although these calculations concern an isolated base and are not involved in nucleic acid, which is generally connected through the N4 atom to a sugar residue, the results obtained here allow us to have a new insight into the structural tautomer interconversion of uracil induced by proton transfer. Such a phenomenon for water molecules in different regions of uracil having stabilization or mutagenicity on uracil could provide an incentive for the future development of the research on the tautomerism of uracil and related gene mutation.

Acknowledgment. This work was supported by the National Natural Science Foundation of China (29976035) and the Zhejiang Provincial Natural Science Foundation of China (RC01051).

Supporting Information Available: The Z-MATRIX of calculated results. This material is available free of charge via the Internet at http://pubs.acs.org.

References and Notes

(1) Watson, J. D.; Crick, F. H. *Nature* **1953**, *171*, 737.
(2) Topal, M. D.; Fresco, J. R. *Nature* **1976**, *263*, 285.
(3) Les, A.; Adamowicz, L. *J. Phys. Chem.* **1989**, *93*, 7078.
(4) Kryachko, E. S.; Nguyen, M. T.; Zeegers-Huyskens, T. *J. Phys. Chem. A* **2001**, *105*, 1288.
(5) Holbrook, S. R.; Cheong, C.; Kim, S. H. *Nature* **1991**, *353*, 579.
(6) Shi, K.; Wahl, M.; Sundaralingam, M. *Nucleic Acids Res.* **1999**, *27*, 2196.
(7) Tsuchiya, Y.; Tamura, T.; Fujii, M.; Ito, M. *J. Phys. Chem.* **1988**, *92*, 1760.
(8) Brown, R. D.; Godfrey, P. D.; McNaughton, D.; Pierlot, A. P. *J. Am. Chem. Soc.* **1988**, *110*, 2329.
(9) Beak, P.; White, J. M. *J. Am. Chem. Soc.* **1982**, *104*, 7073.
(10) Chahinian, M.; Seba, H. B.; Ancian, B. *Chem. Phys. Lett.* **1998**, *285*, 337.
(11) Gaigeot, M.-P.; Leulliot, N.; Ghomi, M.; Jobic, H.; Coulombeau, C.; Bouloussa, O. *Chem. Phys.* **2000**, *261*, 217.
(12) Desfranc, O. C.; Abdoul-Carime, H.; Schermann, J. P. *J. Chem. Phys.* **1996**, *104*, 7792.
(13) Hendricks, J. H.; Lyapustina, S. A.; Clercq, H. L.; Bowen, K. H. *J. Chem. Phys.* **1998**, *108*, 8.
(14) Rybak, S.; Szalewicz, K. *Chem. Phys. Lett.* **1992**, *199*, 567.
(15) Smets, J.; McCarthy, W. J.; Adamowicz, L. *J. Phys. Chem*. **1996**, *100*, 14655.
(16) Smets, J.; Smith, D.-M. A.; Elkadi, Y.; Adamowicz, L. *J. Phys. Chem. A* **1997**, *101*, 9152.
(17) Nguyen, M. T.; Chandra, A. T.; Zeegers-Huyskens, T. *J. Chem. Soc., Faraday Trans.* **1998**, *94*, 1277.
(18) Ghomi, M.; Aamouche, A.; Cadioli, B.; Berthier, G.; Grajcar, L.; Baron, M. H. *J. Mol. Struct.* **1997**, *410*−*411*, 323.
(19) Aamouche, A.; Berthier, G.; Cadioli, B.; Gallinella, E.; Ghomi, M. *J. Mol. Struct.* (*THEOCHEM*) **1998**, *426*, 307.
(20) van Mourik, T.; Price, S. L.; Clary, D. C. *J. Phys. Chem. A* **1999**, *103*, 1611.
(21) van Mourik, T.; Benoit, D. M.; Price, S. L.; Clary, D. C. *Phys. Chem. Chem. Phys.* **2000**, *2*, 1281.
(22) van Mourik, T. *Phys. Chem. Chem. Phys*. **2001**, *3*, 2886.
(23) Dolgounitcheva, O.; Zakrzewski, V. G.; Ortiz, J. V. *J. Phys. Chem. A* **1999**, *103*, 7912.
(24) Gadre, S. R.; Babu, K.; Rendell, A. P. *J. Phys. Chem. A* **2000**, *104*, 8976.
(25) Gaigeot, M.-P.; Ghomi, M. *J. Phys. Chem. B* **2001**, *105*, 5007.
(26) Gaigeot, M.-P.; Kadri, C.; Ghomi, M. *J. Mol. Struct.* **2001**, *565*−*566*, 469.
(27) Palafox, M. A.; Iza, N.; Gil, M. *J. Mol. Struct. (THEOCHEM)* **2002**, *585*, 69.
(28) Zhang, R. B.; Zhang, X. D.; Qu, Z. W.; Ai, X. C.; Zhang, X. K.; Zhang, Q. Y. *J. Mol. Struct. (THEOCHEM)* **2003**, *624*, 169.
(29) Gaigeot, M.-P.; Sprik, M. *J. Phys. Chem. B* **2003**, *107*, 10344.
(30) Gaigeot, M.-P.; Sprik, M. *J. Phys. Chem. B* **2004**, *108*, 7458.
(31) Jalbout, A. F.; Hall-Black, C. S.; Adamowicz, L. *Chem. Phys. Lett.* **2002**, *354*, 128.
(32) Smith, D. M.; Smets, J.; Adamowicz, L. *J. Phys. Chem. A* **1999**, *103*, 5784.
(33) Kryachko, E.; Nguyen, M. T.; Zeegers-Huyskens, T. *J. Phys. Chem. A* **2001**, *105*, 3379.
(34) Kryachko, E.; Nguyen, M. T.; Zeegers-Huyskens, T. *Chem. Phys.* **2001**, *264*, 21.
(35) Stepanian, S. G.; Jalbout, A. F.; Hall, C. S.; Adamowicz, L. *J. Phys. Chem. A* **2003**, *107*, 7911.
(36) Orozco, M.; Hernández, B.; Luque, F. J. *J. Phys. Chem. B* **1998**, *102*, 5228.
(37) Tian, S. X.; Zhang, C. F.; Zhang, Z. J.; Chen, X. J.; Xu, K. Z. *Chem. Phys.* **1999**, *242*, 217.
(38) Kryachko, E. S.; Nguyen, M. T.; Zeegers-Huyskens, T. *J. Phys. Chem. A* **2001**, *105*, 1934.
(39) Hocquet, A.; Leulliot, N.; Ghomi, M. *J. Phys. Chem. B* **2000**, *104*, 4560.
(40) Malick, D. K.; Petersson, G. A. *J. Chem. Phys.* **1998**, *108*, 5704.
(41) Peiró-García, J.; Nebot-Gil, I. *ChemPhysChem* **2003**, *4*, 843.
(42) Boys, S. F.; Bermardi, F. *Mol. Phys.* **1970**, *19*, 553.
(43) Kulkarni, A. D.; Babu, K.; Gadre, S. R.; Bartolotti, L. J. *J. Phys. Chem. A* **2004**, *108*, 2492.
(44) Frisch, M. J.; Trucks, G. W.; Schlegel, H. B.; Scuseria, G. E.; Robb, M. A.; Cheeseman, J. R.; Zakrzewski, V. G.; Montgomery, J. A., Jr.; Stratmann, R. E.; Burant, J. C.; Dapprich, S.; Millam, J. M.; Daniels, A. D.; Kudin, K. N.; Strain, M. C.; Farkas, O.; Tomasi, J.; Barone, V.; Cossi, M.; Cammi, R.; Mennucci, B.; Pomelli, C.; Adamo, C.; Clifford, S.; Ochterski, J.; Petersson, G. A.; Ayala, P. Y.; Cui, Q.; Morokuma, K.; Malick, D. K.; Rabuck, A. D.; Raghavachari, K.; Foresman, J. B.; Cioslowski, J.; Ortiz, J. V.; Stefanov, B. B.; Liu, G.; Liashenko, A.; Piskorz, P.; Komaromi, I.; Gomperts, R.; Martin, R. L.; Fox, D. J.; Keith, T.; Al-Laham, M. A.; Peng, C. Y.; Nanayakkara, A.; Gonzalez, C.; Challacombe, M.; Gill, P.-M. W.; Johnson, B.; Chen, W.; Wong, M. W.; Andres, J. L.; Gonzalez, C.; Head-Gordon, M.; Replogle, E. S.; Pople, J. A. *Gaussian 98*, revision A.3; Gaussian, Inc.: Pittsburgh, PA, 1998.
(45) Huyskens, P. L. *J. Am. Chem. Soc.* **1977**, *99*, 2578.
(46) Stewart, R. F.; Jensen, L. H. *Acta Crystallogr*. **1967**, *23*, 1102.
(47) Ferenczy, G.; Harsany, L.; Rozsondai, B.; Hargittai, I. *J. Mol. Struct.* **1986**, *140*, 71.
(48) Florián, J.; Leszczyński, J. *J. Am. Chem. Soc.* **1996**, *118*, 3010.
(49) Guallar, V.; Douhal, A.; Moreno, M.; Lluch, J. M. *J. Phys. Chem. A* **1999**, *103*, 6251.
(50) Marshall, J. R.; Walker, J. *J. Chem. Soc.* **1951**, 1005.
(51) Katritzky, A. R.; Waring, A. J. *J. Chem. Soc.* **1962**, 1540.
(52) Berg, J. M.; Tymoczko, J. L.; Stryer, L.; Clarke, N. D. *Biochemistry;* W. H. Freeman: New York, 2002. This book is available via the Internet at http://www.ncbi.nlm.nih.gov/.
(53) Sowers, L. C.; Goodman, M. F.; Eritja, R.; Kaplan, B.; Fazakerley, G. V. *J. Mol. Biol.* **1989**, *205*, 437.
(54) Sowers, L. C.; Eritja, R.; Kaplan, B.; Goodman, M. F.; Fazakerley, G. V. *J. Biol. Chem.* **1988**, *263*, 14794.
(55) Bohr, F.; Henon, E. *J. Phys. Chem. A* **1998**, *102*, 4857.
(56) Isaacson, A. D.; Truhlar, D. G. *J. Chem. Phys.* **1982**, *76*, 1380.
(57) Soto, M. R. *J. Phys. Chem.* **1995**, *99*, 6540.
(58) Reed, A. E.; Curtiss, L. A.; Weinhold, F. *Chem. Rev.* **1988**, *88*, 899.